Chapter 26

BINARY ACTUATION

Jean-Sébastien Plante and Steven Dubowsky

[AQ1] *Massachusetts Institute of Technology, Cambridge, MA, USA*

Abstract

Binary actuation is a robotic and mechatronic system design paradigm that uses a large number (10 to 1000s) of binary actuators. Each actuator typically has two stable states that do not need power to be maintained. Binary system actuators need to be lightweight, low cost, and to have good performance, such as dielectric elastomer actuators (DEAs). A key characteristic of DEAs is that their performance and reliability is highly dependent on stretch rate. In particular, their maximum safe extension increases significantly when operated at high stretch rates. Binary actuation exploits this property by using DEAs intermittently at high speeds for switching state. This chapter explains the basics of binary actuation using DEAs. Two examples of the application of DEAs to binary devices are discussed: a manipulator for intra-magnetic resonance imaging (MRI) medical interventions and a hopping robot for space exploration. These examples suggest that binary actuation using DEAs is practical even with current actuator performance.

Keywords: Actuator, binary, bi-stable, dielectric, discrete, elastomer, hop, magnetic, manipulator, mechatronic, medical, MR, resonance, robotic, space.

26.1 INTRODUCTION

Many robotic and mechatronic systems and devices would greatly benefit from a design paradigm called *binary actuation*[1–4]. Binary actuation can be thought of as the mechanical analogue of digital electronics where each actuator ‘flips’ between one of two discrete states. Such systems would be simple, robust, lightweight, inexpensive, and easy to control. Figure 26.1 illustrates a simple 3-degree-of-freedom (DOF) binary device in each of its $2^3 = 8$ positions [5]. Systems design and control is greatly simplified since low-level feedback control is virtually eliminated, along with the associated sensors, wiring, and electronics [6].

Simulations have shown that binary robotics devices are kinematically capable of executing practical tasks, such as instrument placement for planetary exploration, legged locomotion through rough terrain, and industrial and medical devices (see Fig. 26.2) [7, 8]. Studies suggest that less than 100 binary DOF will provide sufficient resolution for many practical tasks, and that the associated computing requirements for solving their inverse kinematics are reasonable [5, 7].

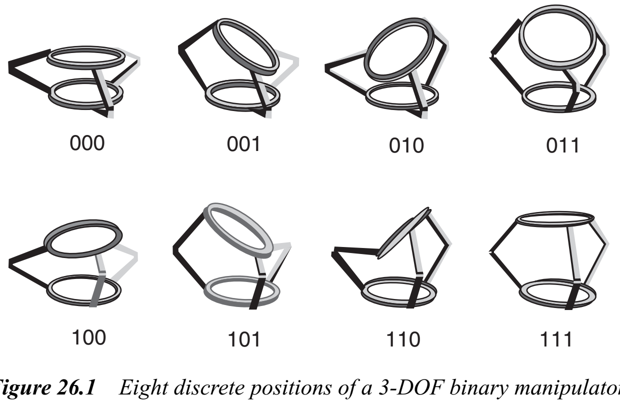

Figure 26.1 *Eight discrete positions of a 3-DOF binary manipulator.*

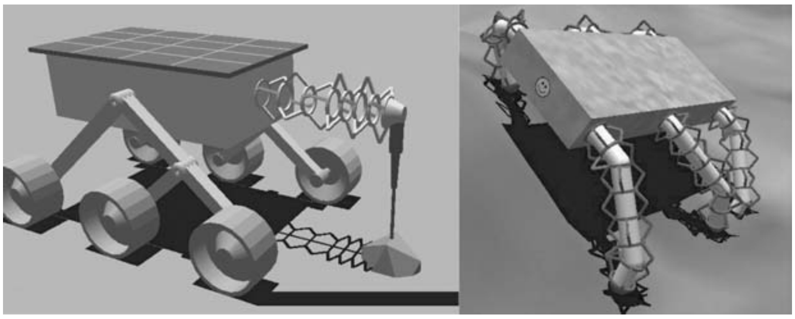

Figure 26.2 Example of binary robotic applications: (a) manipulator on a conventional rover and (b) legs of a walking robot.

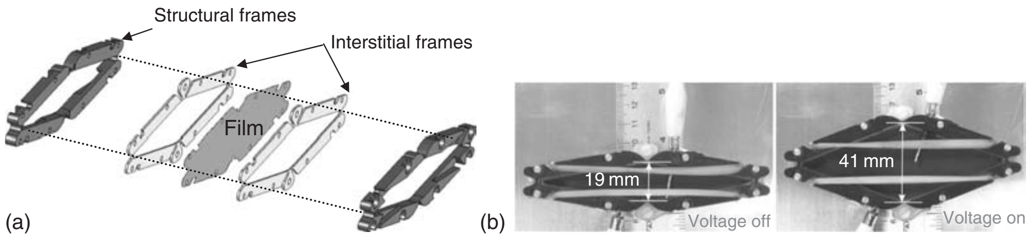

Figure 26.3 DEA with linear extensions greater than 100%: (a) exploded view and (b) prototype.

To date, the primary challenge to implementing practical large-DOF binary robotic systems has been the development of effective binary actuators. Conventional actuators are too expensive, heavy, and complex to be used in large numbers. This chapter explores the strengths and limitations of bi-stable dielectric elastomer actuators (DEAs) technology as applied to robotic and mechatronic systems and devices. It is shown that these actuators are particularly well suited to binary actuation.

Under laboratory conditions, DEAs have shown substantial energy densities (actuator mechanical work per unit mass of actuator), significantly exceeding those of conventional technologies such as electromagnets [9–11]. DEAs are potentially a key enabling technology for large-DOF binary robotic devices with their linear extensions of more than 100% (see Fig. 26.3). They are lightweight and simple compared to conventional actuators. They can be implemented in large numbers without complex motion amplification transmissions [8, 12].

Reliability has been found to be an important problem of DEAs. For example, actuators based on VHB 4905/4910 have experienced high 'infant mortalities' and short shelf lives, particularly when high performance is required [13]. Most importantly, these actuators experienced erratic and misunderstood failures during operation [13, 14].

Recent studies of DEAs failure modes, have shown, by experimentally validated continuum mechanics models that the failure modes of DEAs change dramatically with stretch rate (or actuator speed) due to their viscoelastic character [15]. A failure mode, called pull-in failure, significantly limits actuator extension at low stretch rates but not at high stretch rates. Thus DEAs can be reliable at high actuation rate, making them compatible with bi-stable binary actuation where they are only powered intermittently while changing positions between states. It is shown here that given these characteristics, practical robotic devices based on bi-stable DEAs can be developed. Two applications are discussed: a 7-DOF binary manipulator and a hopping robot for planetary exploration.

26.2 BINARY ACTUATORS

Since a relatively large number of actuators are generally required for binary systems, to be practical, these actuators must be simple and low cost. Furthermore, binary actuators should have relatively high forces and work outputs for their weight, acceptable energy conversion efficiencies, and be capable

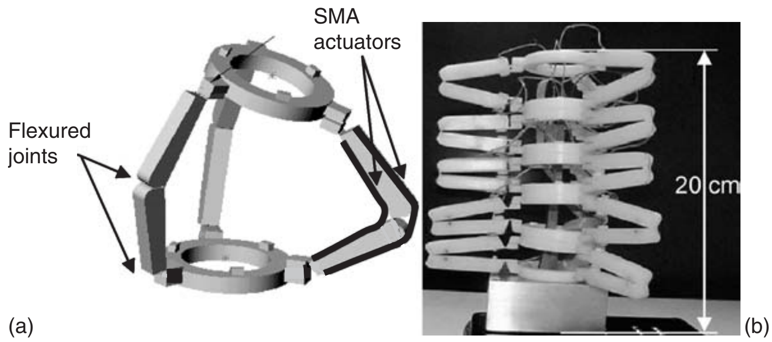

Figure 26.4 *The MIT SMA powered binary manipulator [18]: (a) single-stage and (b) five-stage devices.*

to operate at acceptable speeds. Conventional actuators, such as DC motors and pneumatic cylinders, while well suited for conventional systems, are too heavy and complex for binary actuation [16, 17].

In recent years, new actuation technologies have been developed. However, these have limited use for binary systems [16]. Shape memory alloys (SMA) rely on volume contractions driven by alloy phase changes (see Fig. 26.4). They are relatively slow, limited to low efficiencies, and sensitive to environment temperature. Ionic polymers (conducting polymers) change volume when their polymer chains absorb or swell ions. Such systems must be kept in aqueous environments, are slow, and while have good force output, their extensions are very small. Piezoelectric materials are relatively heavy and also have very small extensions. Hence, both piezoelectric and ionic polymers require complex transmissions for many practical applications such as binary actuation. Optimized linear electromagnetic systems (solenoids) can experience overheating issues and are heavy.

DEAs have been proposed to replace conventional actuators. They have good performance characteristics and are inherently inexpensive [19, 20]. However, as continuous actuators, their practical implementation has been limited by their problematic reliability and efficiency. As discussed below, those limitations can be avoided in properly designed binary systems.

26.3 PROPERTIES OF DEAs

An experimentally validated analytical model of the failure modes of DEAs has recently been developed [15]. A brief summary of this model is presented in Section 26.6. The model considers three failure modes: material strength, dielectric strength, and pull in. Pull-in failure is an unstable condition that can occur when the Maxwell pressure becomes always greater than the film compressive stress. Model predictions are compared with experimental data of 10 identical diamond actuators (see Fig. 26.3) built with 3Ms VHB 4905/4910 elastomer. The actuators were all tested at the same pre-stretch area expansion of about 11 because this value was found to offer optimum performance [15]. The samples were first tested at a high stretch rate that is typical of many DEA applications (~10 s to reach 100% extension). No failure was observed. The same samples were then tested at a low stretch rate where viscoelastic effects are negligible such as when an actuator holds its position for extended periods of time (~1 h to reach 100% extension). All 10 actuators failed. The data is presented in Fig. 26.5 where actuator area expansion, $\lambda^2_{1,\mathrm{act}}$, is plotted versus pre-stretch area expansion, $\lambda^2_{1,\mathrm{pre}}$. At high stretch rates, the actuators were pulled up to area expansion of 2.27 (150% linear extension) without failure, as predicted by the model. At low stretch rates, failure was caused by pull-in at an average area expansion of 1.28 (30% linear strain) with a lowest value of 1.05 (6% linear strain). As shown by Fig. 26.5, the analytical predictions corroborate well with the experimental data.

The differences between the low and high stretch rate failure behaviour are explained by the fundamental role of viscoelasticity on actuator failure. At high stretch rates, the viscous forces ‘stiffen’ the film and protect it from pull-in failures. In contrast, low stretch rates generate less viscous impedance and pull-in failures dominate. The conclusion of this study is that, to achieve long life and good reliability, DEAs must be used at high stretch rate where viscoelastic forces prevent pull-in failure.

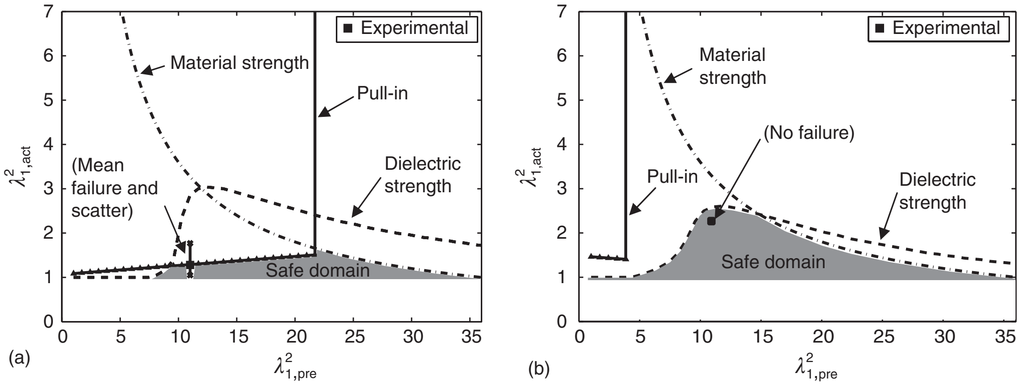

Figure 26.5 *Failure analytical predictions for (a) low stretch rate ($\dot{\lambda}_{uni} = 3.3\times10^{-4}\,s^{-1}$) and (b) high stretch rate ($\lambda_{uni} = 0.0945$) with loading stress [15].*

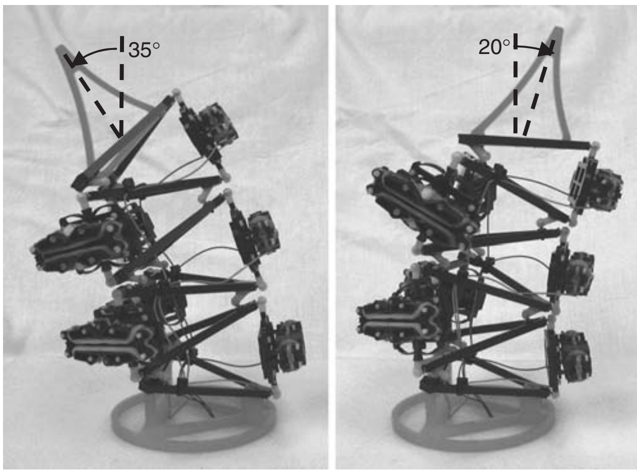

Figure 26.6 *A 7-DOF binary manipulator prototype.*

It is fortuitous that reliable DEAs operation occurs at high speeds, precisely as required for bi-stable binary actuation where actuators are only used at high stretch rates during state switching and are otherwise unpowered. This strategy not only matches well with the reliability requirement but also significantly improve efficiency by minimizing current leakage losses [21]. Two examples of binary robotic devices are discussed below.

26.4 BINARY ROBOTIC SYSTEMS WITH DEAs

26.4.1 Binary manipulation

A proof of concept of a 7-DOF binary manipulator is shown in Fig. 26.6 [22]. This snake-like device demonstrates the large displacement capabilities of DEAs with a tip angle range of 55°, using only two and a half stages. Such all-polymer manipulators could be used for low-force (~5 N) medical interventions inside magnetic resonance imaging (MRI) environments since DEAs have been demonstrated to be MRI compatible [8].

The simplest strategy to design a bi-stable module for binary manipulators is to use an antagonistic pair of actuators that 'flip' the state of a bi-stable element. An exploded view of a 1-DOF antagonistic module is shown in Fig. 26.7(a). Figure 26.7(b) shows a prototype playing 'pool' with a plastic cylinder (the cylinder looks blurry because it is in motion) [12]. In the figure, DEA 1 is completing an opening

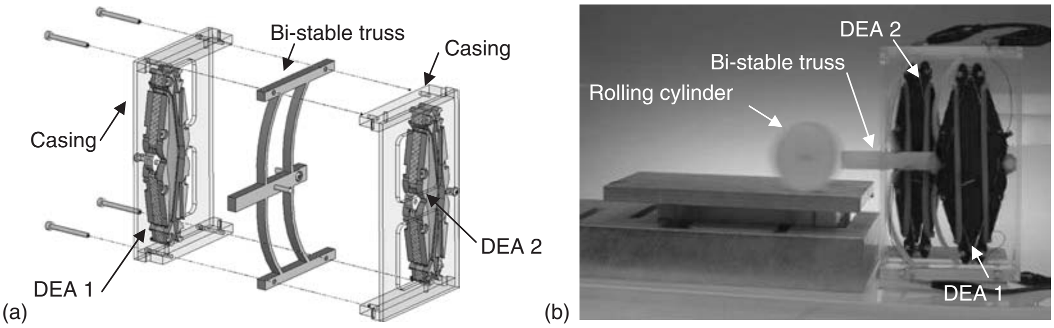

Figure 26.7 *Antagonistic bi-stable module: (a) exploded view and (b) prototype.*

Table 26.1 *Bistable module specifications.*

Performance Metrics	Antagonistic Actuators (at 1.6 mm/s)	Single Actuator (at 0.8 mm/s)
Displacement	25 mm	13 mm
Strain	30%	35%
Force (min/max)	1–3 N	1–3.5 N
Mass	220 g	16.4 g
Force-to-weight	0.46	6
Work output	1.14×10^{-4} J/g	0.0015 J/g
Switching time	~5 s	~5 s
Size (closed)	135 × 81 × 48 mm	65 × 35 × 22 mm

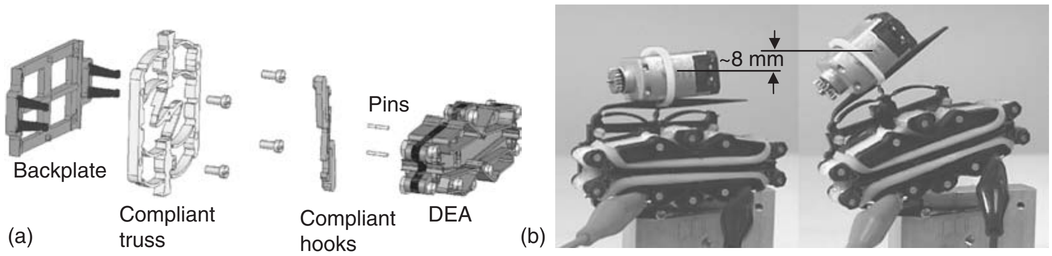

Figure 26.8 *Bi-stable module using a single actuator: (a) exploded view and (b) prototype.*

cycle and is thus showed in an extended state. The bi-stable truss has been switched to the left, which set the plastic cylinder in motion. Firing DEA 2 would switch the bi-stable truss back to the right. The performance specifications of this prototype are shown in Table 26.1.

A second strategy to implement bi-stable DEAs is to couple a single DEA with a compliant indexing transmission (see Fig. 26.8) [22]. The 16.4 g bi-stable module is shown switching a 25 g DC motor up and down. These same modules were used for the manipulator of Fig. 26.6. The performance specifications are shown in Table 26.1. The single actuator device is more compact, has better force-to-weight characteristics, but is more complex than the antagonistic pair actuator. Each of the binary modules discussed so far could be used in low-DOF binary applications such as, for example, automotive door locks and trunk release, general HVAC control, and industrial pick-and-place tasks.

26.4.2 Space exploration robots locomotion

A proposed mission concept for planetary exploration is based on the deployment of a large number of small hopping Microbots over vast areas of a planet's surface and subsurface, including features such as caves and craters (see Fig. 26.9). This would allow extremely large-scale in situ analysis of the terrain.

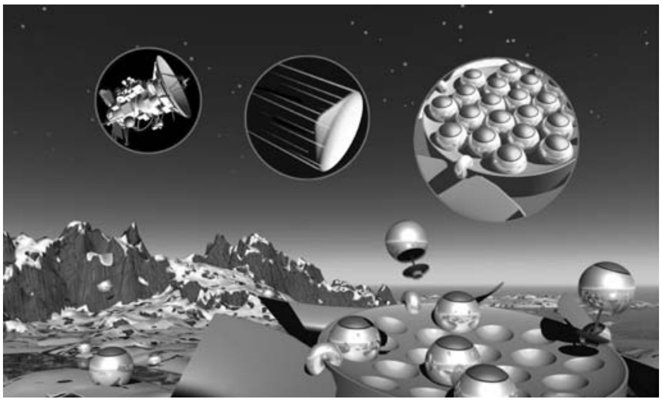

Figure 26.9 Microbot mission concept (rendering by Gus Frederick).

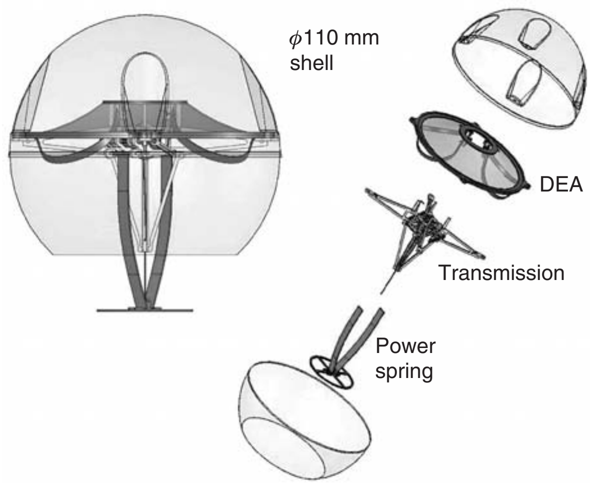

Figure 26.10 Microbot mobility concept.

A Microbot's mobility concept consists in pumping mechanical energy generated by a DEA into a power spring via a ratcheting transmission (see Fig. 26.10). Each pumping cycle moves the power spring in a new stable state, each time raising the system's potential energy. After a certain number of pumping cycles, the stored energy is quickly released to make the system hop. A 26 g Microbot prototype performed tethered hops of about 60 cm after cranking a carbon fiber leaf spring in 35 discrete actuator pumps (see Fig. 26.11). The discrete states are maintained by a ratcheting transmission using a pair of miniature needle clutch bearings. Such applications could be thought of as multi-stable actuation.

26.5 CONCLUSION

The simple, low cost, lightweight, and high performance DEAs are shown to be effective in binary robotic and mechatronic systems and devices. At the same time, bi-stable binary actuation allows DEAs to operate at high stretch rates where they show good performance and reliability. The marriage of DEAs and binary robotics is very harmonious.

Application examples of DEAs to binary manipulation have been discussed through a binary manipulator and a hopping robot using multi-stable energy pumping. The performance of bi-stable DEAs is superior to previous alternative technologies such as electromagnetics, SMAs, and ionic polymers.

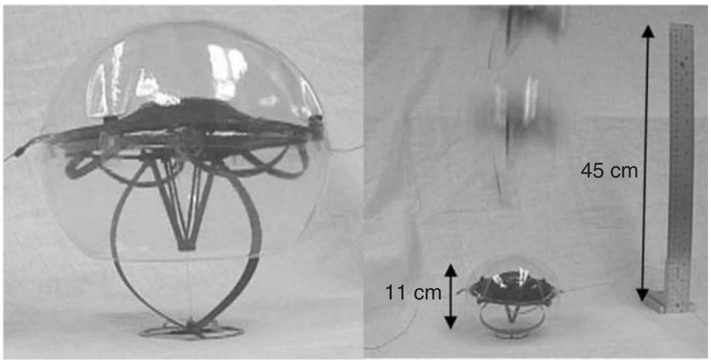

Figure 26.11 *Microbot prototype performing hops of 60 cm.*

However, binary actuation using current DEAs still requires improvement, particularly in terms of actuator force-to-weight ratio. This is likely to happen in a near future with new material development and improved manufacturing methods. Also, improved binary manipulator design using elastically average actuators are currently under development. Such redundant parallel manipulators are likely to be stiffer and have larger forces than conventional serial chains.

26.6 APPENDIX: SUMMARY OF DEA FAILURE MODES STUDY

Three failure modes are considered:

1. Material strength failure occurs when folded polymer chains are straightened beyond their unfolded length. Hence, it is primarily a function of stretch. Experiments have shown that film area expansion of 36 is a reasonable limit [23]. Failure occur when:

$$\lambda_{1,\mathrm{tot}}^2 > 36 \tag{26.1}$$

2. Dielectric strength failure is obtained from experimental breakdown voltage versus total stretch data. Failure occurs when the electric field is higher than the experimental dielectric strength:

$$E > E_{\mathrm{exp}}(\lambda_{1,\mathrm{tot}}) \tag{26.2}$$

3. Pull-in failure instability appears when an equilibrium between the applied equivalent Maxwell pressure (P) and the film compressive stress ($\sigma_{3,\mathrm{act}}$) cannot be reached. The film collapses into highly complex 3D wrinkling patterns leading to failure from either dielectric or material breakdown.

An analytical model used to study the failure modes is developed by considering a small conductive circle coated on both side of a large pre-stretched film fixed on rigid rings (see Fig. 26.12). Under Maxwell pressure resulting from voltage application, the circle's radius increases from its pre-stretched value, r_{pre}, to its actuated value, r_{act}. The film deformation occurs largely away from the film's rigid ring ($r_{\mathrm{rig}} > r_{\mathrm{act}}$) and local failure modes are minimized, putting emphasis on fundamental material failure modes. The effect of external work is considered by imposing a radial load stress acting against the expanding circle and whose numerical value is estimated on diamond actuators.

The film is modelled as a hyperelastic material. Viscoelastic effects are included by defining different elastic material models at different, constant stretch rates.

The deformation of the active region (expanding circle) is illustrated in Fig. 26.13. The deformation is decomposed into two consecutive deformations: the pre-stretch deformation and the actuation deformation. The dimensions in the reference configuration (prior to pre-stretch) are expressed in the R, Θ, Z system. The dimensions in the pre-stretched and actuated dimensions are expressed in the r, θ, z coordinates. The pre-stretch deformation is due to the stretching of the film prior to actuation. It consists of imposed equibiaxial deformations that produce principal stresses in the pre-stretched configuration, $\sigma_{1,\mathrm{pre}}$, $\sigma_{2,\mathrm{pre}}$, $\sigma_{3,\mathrm{pre}}$. The pre-stretched configuration is then perturbed by the equivalent Maxwell pressure,

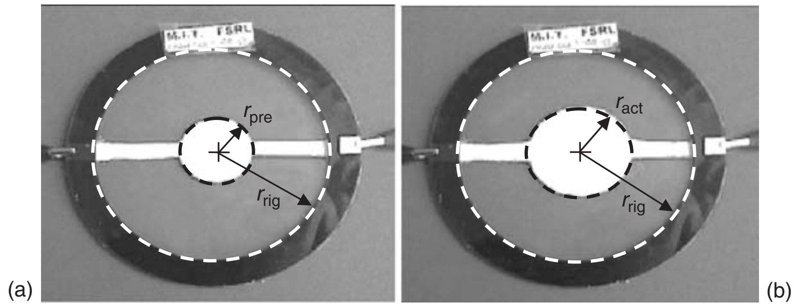

Figure 26.12 *Expanding circle: (a) pre-stretched (V = 0 kV) and (b) actuated (V = 10 kV).*

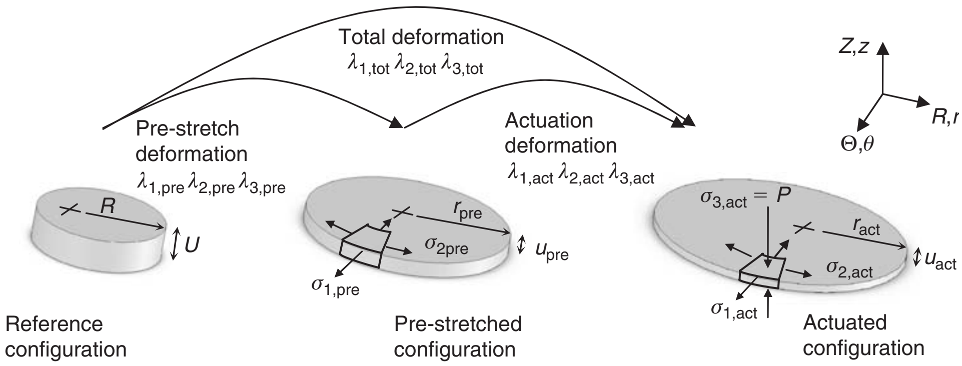

Figure 26.13 *The deformations and stresses of the active region.*

P, resulting from voltage application. The film further deforms and the stresses in the actuated configuration reach a new equilibrium to $\sigma_{1,act}$, $\sigma_{2,act}$, $\sigma_{3,act}$.

The Maxwell stresses are expressed by an equivalent Maxwell pressure, P, given in references [24]:

$$P = -\varepsilon_d \varepsilon_0 \left(\frac{V}{u_{act}} \right)^2 \tag{26.3}$$

where ε_0 is the free-space permittivity, ε_d is the material's dielectric constant, V is the voltage applied across the electrodes, and u_{act} is the actuated film thickness.

The objective of the model is to find the actuation stretches, $\lambda_{i,act}$, for any given voltage, V, mechanical pre-stretch, $\lambda_{i,pre}$, stretch rate of the uniaxial test used to define the elastomer constitutive model, $\dot{\lambda}_{uni}$, and load, σ_{load}:

$$\lambda_{i,act} = f(V, \lambda_{i,pre}, \dot{\lambda}_{uni}, \sigma_{load}) \quad i = 1,\ 2,\ 3 \tag{26.4}$$

The actuation stretch, $\lambda_{i,act}$, is reached when the equivalent Maxwell pressure, P, of Eq. (26.1) is in equilibrium with the film's axial stress:

$$P(V, \lambda_{1,pre}, \lambda_{1,act}) = \sigma_{3,act}(\lambda_{1,pre}, \lambda_{1,act}, \sigma_{load}) \tag{26.5}$$

The axial stress, $\sigma_{3,act}$, is found from a stress/stretch model based on Ogden's formulation [25] given by:

$$\sigma_{3,act} = \sigma_{1,act} - \mu_1(\lambda_{1,tot})^{\alpha_1} - \mu_2(\lambda_{1,tot})^{\alpha_2} + \mu_1(\lambda_{3,tot})^{\alpha_1} + \mu_2(\lambda_{3,tot})^{\alpha_2} \tag{26.6}$$

The film planar stress, $\sigma_{1,act}$, includes the stress due to the deformation of the film's passive region and the effect of a load stress estimated from experimental measurements taken on diamond actuators [15].

References

[1] Pieper, D. L. (1968). The kinematics of manipulators under computer control. Ph.D. Dissertation, Stanford University, Palo Alto, CA.

[AQ2] [2] Roth, B., Rastegar, J. and Scheinman, V. (1973). On the design of computer controlled manipulators. *First CISM-IFTMM Symposium on Theory and Practice of Robots and Manipulators*, pp. 93–113.

[AQ3] [3] Chirikjian, G. (1994). A binary paradigm for robotic manipulators. *Proceedings of the 1994 IEEE International Conference on Robotics and Automation*, Vol. 4, pp. 3063–3069.

[4] Lees, D. and Chirikjian, G. (1996). A combinatorial approach to trajectory planning for binary manipulators. *Proceedings of the 1996 IEEE International Conference on Robotics and Automation*, Minneapolis, MN.

[5] Lichter, M. D., Sujan, V. A. and Dubowsky, S. (2000). Experimental demonstrations of a new design paradigm in space robotics. *International Symposium on Experimental Robotics (ISER '00)*, Honolulu, HI.

[AQ4] [6] Goldberg, K. (1992). Orienting polygonal parts without sensors. *Algorithmica, Special Robotics Issue*.

[7] Lichter, M., Sujan, V. and Dubowsky, S. (2002). Computational issues in the planning and kinematics of binary robots. *Proceedings of the 2002 IEEE International Conference on Robotics and Automation*, Washington, DC.

[AQ3] [8] Vogan, J., Wingert, A., Hafez, M., Plante, J. S., Dubowsky, S., Kacher, D. and Jolesz, F. (2004). Manipulation in MRI devices using electrostrictive polymer actuators: with an application to reconfigurable imaging coils. *Proceedings of the 2004 IEEE International Conference on Robotics and Automation*, pp. 2498–2504.

[AQ3] [9] Kornbluh, R., Pelrine, R. and Joseph, J. (1995). Elastomeric dielectric artificial muscle actuators for small robots. *Proceedings of the Materials Research Society Symposium*, Vol. 600, pp. 119–130.

[10] Kornbluh, R., Pelrine, R., Pei, Q., Oh, S. and Joseph, J. (2000). Ultrahigh strain response of field-actuated elastomeric polymers. *Smart Structures and Materials 2000 (EAPAD)*, *Proc. SPIE*, **3987**, 51–64.

[11] Wingert, A., Lichter, M. D. and Dubowsky, S. (2006). On the design of large degree-of-freedom digital mechatronic devices based on bistable dielectric elastomer actuators. *IEEE/ASME Trans. Mechatron.*, **11**, 448–456.

[AQ3] [12] Plante, J. S., Dubowsky, S., Santer, M. and Pellegrino, S. (2005). Compliant bistable dielectric elastomer actuators for binary mechatronic systems. *Proceedings of the ASME International Design Engineering Technical Conference/29th Mechanisms and Robotics Conference*, Vol. 7A, pp. 121–126.

[13] Vogan, J. (2004). Development of dielectric elastomer actuators for MRI devices. M.S. Thesis, Department of Mechanical Engineering, Massachusetts Institute of Technology, Cambridge, MA.

[14] Wingert, A. (2002). Development of a polymer-actuated binary manipulator. M.S. Thesis, Department of Mechanical Engineering, Massachusetts Institute of Technology, Cambridge, MA.

[AQ5] [15] Plante, J. S. and Dubowsky, S. (2006). Large-scale failure modes of dielectric elastomer actuators. *Int. J. Solids Struct.*, in press.

[16] Hafez, M., Lichter, M. D. and Dubowsky, S. (2003). Optimized binary modular reconfigurable robotic devices. *IEEE/ASME Trans. Mechatron.*, **8**, 18–25.

[17] Chirikjian, G. and Burdick, J. (1991). Hyper-redundant robotic mechanisms and their applications. *IEEE/RSJ International Workshop on Intelligent Robots and Systems*, Osaka, Japan.

[AQ3] [18] Sujan, V., Lichter, M. and Dubowsky, S. (2001). Lightweight hyper-redundant binary elements for planetary exploration robots. *Proceedings of IEEE/ASME International Conference on Advanced Intelligent Mechatronics*, Vol. 2, pp. 1273–1278.

[19] Pelrine, R., Sommer-Larsen, R., Kornbluh, R., Heydt, R., Kofod, G., Pei, Q. and Gravesen, P. (2001). Applications of dielectric elastomer actuators. *Smart Structures and Materials 2001 (EAPAD)*, *Proc. SPIE*, **4329**, March 2001.

[20] Meijer, K., Rosenthal, M. and Full, R. J. (2001). Muscle-like actuators? A comparison between three electroactive polymers. *Smart Structures and Materials 2001 (EAPAD)*, *Proc. SPIE*, **4329**, 7–15.

[AQ5] [21] Plante, J. S. and Dubowsky, S. (2006). On the properties of dielectric elastomer actuators and its implications for their design. *J. Smart Mater. Struct.*, to be published.

[22] Plante, J. S. (2006). Dielectric elastomer actuators for binary robotics and mechatronics. Ph.D. Dissertation, Department of Mechanical Engineering, Massachusetts Institute of Technology, Cambridge, MA.

[23] Kofod, G., Kornbluh, R., Pelrine, R. and Sommer-Larsen, P. (2001). Actuation response of polyacrylate dielectric elastomers. *Smart Structures and Materials 2001 (EAPAD)*, *Proc. SPIE*, **4329**, 141–147.

[24] Pelrine, R., Kornbluh, R. and Joseph, J. (1998). Electrostriction of polymer dielectrics with compliant electrodes as means of actuations. *Sens. Act. A Phys.*, **64**, 77–85.

[25] Ogden, R. W. (1982). Elastic deformations of rubberlike solids. *Mechanics of Solids*. Pergamon Press, Oxford, pp. 499–537.

Author Queries

{AQ1} Please provide Department for the authors affliation and also note that for the affiliation of author 'Jean-Sébastien Plante' we have followed MSS.
{AQ2} Please provide the place of symposium for reference [2].
{AQ3} Please provide the place of proceedings for references [3], [8], [9], [12], [18].
{AQ4} Please provide volume and page range for reference [6].
{AQ5} Please update references [15] and [21].